Volume 51 | Number 14 | 18 February 2015 | Pages 2737–3004

ChemComm

Chemical Communications

www.rsc.org/chemcomm

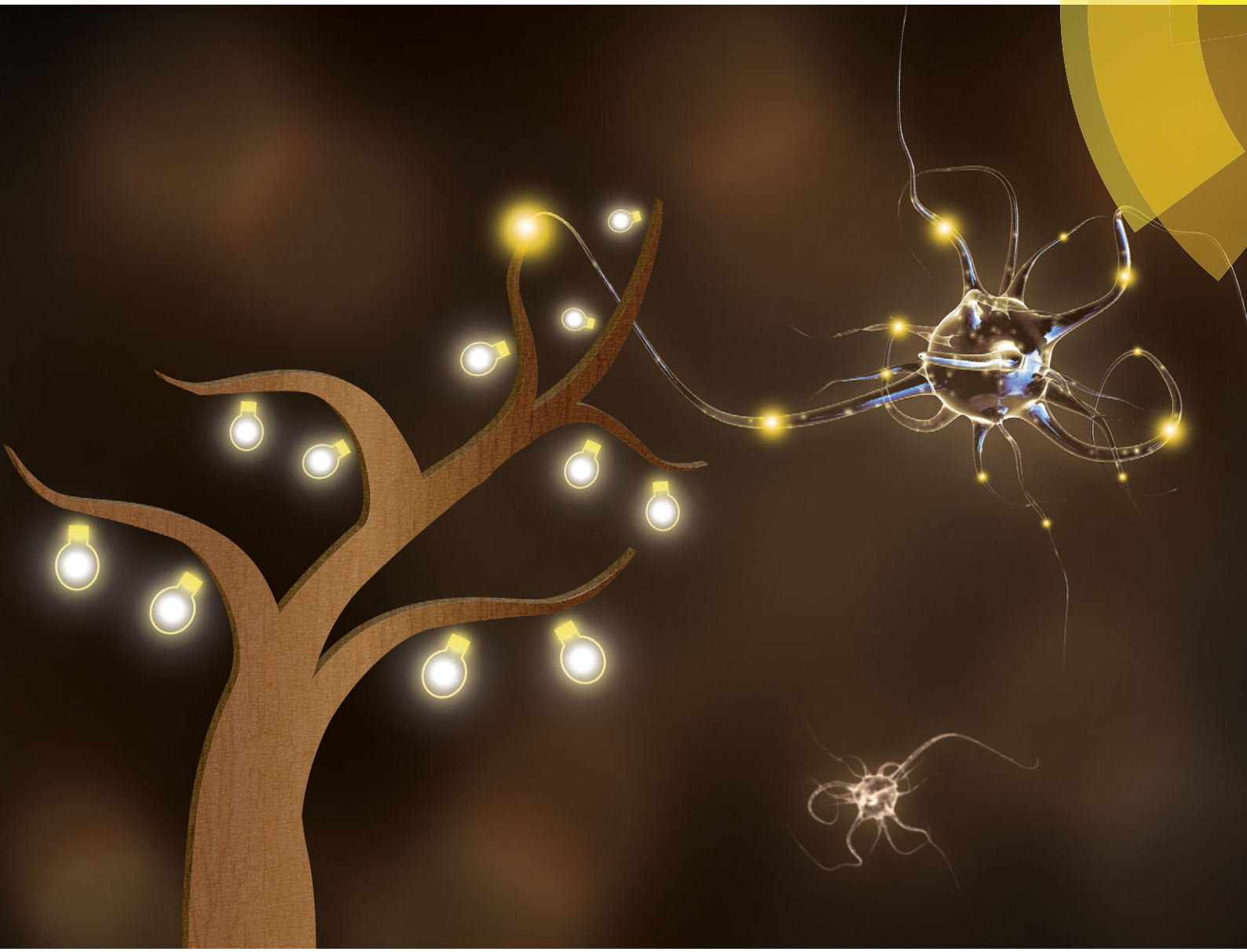

ISSN 1359-7345

ROYAL SOCIETY OF CHEMISTRY

COMMUNICATION

Goran Angelovski *et al.*

Dendrimeric calcium-responsive MRI contrast agents with slow *in vivo* diffusion

ChemComm

COMMUNICATION

View Article Online
View Journal | View Issue

Cite this: *Chem. Commun.*, 2015, 51, 2782

Received 24th September 2014,
Accepted 30th October 2014

DOI: 10.1039/c4cc07540d

www.rsc.org/chemcomm

Dendrimeric calcium-responsive MRI contrast agents with slow *in vivo* diffusion†

Serhat Gündüz,[ab] Nobuhiro Nitta,[c] Sandip Vibhute,[b] Sayaka Shibata,[c] Martin E. Mayer,[d] Nikos K. Logothetis,[be] Ichio Aoki[c] and Goran Angelovski*[a]

We report a methodology which enables the preparation of dendrimeric contrast agents sensitive to Ca^{2+} when starting from the monomeric analogue. The Ca-triggered longitudinal relaxivity response of these agents is not compromised by undertaking synthetic transformations, despite structural changes. The *in vivo* MRI studies in the rat cerebral cortex indicate that diffusion properties of dendrimeric contrast agents have great advantages as compared to their monomeric equivalents.

Smart or responsive contrast agents (SCAs) can have a significant role in magnetic resonance imaging (MRI). These are molecular sensors capable of altering their magnetic properties upon changing their local environment, thus indicating a modification in the physiology of the studied biological system. In turn, SCAs enable the assessment of biological processes *in vivo* at the cellular and molecular levels, with an outstanding spatial and temporal resolution.

A number of SCAs for the use in MRI have been developed so far.[1–3] Nevertheless, their broader application is still pending, with only a few demonstrating their potential *in vivo*.[4–6] In neuroimaging, SCAs enable a new functional MRI (fMRI) method that measures brain function to be developed.[7,8] For this purpose, Ca^{2+} and various neurotransmitter molecules are the most preferred SCA targets due to their critical involvement in neuronal signaling.[5,9]

However, when using SCAs for fMRI, temporally resolved information within the range of seconds is necessary to successfully follow the dynamics of Ca^{2+} transients or neurotransmitter release. In such cases, the ability to compare the signal intensity (SI) from two types of scan series (with and without brain tissue stimulation) is crucial for the success of the fMRI experiment.[5] Principally, one aims to have no or minimal SCA concentration change during the two consecutive experiments, so that the SI change may be associated only with the target concentration change. Otherwise, the inability to control the local SCA concentration may lead to ambiguous results. The recorded MRI signal in T_1- and T_2-weighted imaging depends on the agent concentration and relaxivity (r_1 or r_2 for T_1- or T_2-based SCA, respectively),[2] as well as its background signal (the MR signal of tissue in the absence of an SCA). Therefore, the signal changes are usually a consequence of the SCA concentration change in a particular voxel rather than its relaxivity change, which prevents any conclusions on actual SCA activity. Few attempts to combine quantitative MRI techniques have been made to allow better control of the local SCA concentration.[10–12]

An option to control the SCA concentration and minimize its changes may be by affecting SCA diffusion properties. Our previous studies show that monomacrocyclic conventional contrast agents (Magnevist®, Dotarem®) or Ca-sensitive SCAs diffuse very fast into the rat cerebral cortex, unless Ca-induced aggregation and the resulting increase in the size of the agent causes slower diffusion.[13–15] A fast SI decrease or aggregate formation complicates or completely prevents Ca-dependent fMRI, demanding the optimization of the SCA only beyond the r_1 changes.

We have therefore sought to attach one of our very active Ca-sensitive SCAs to a dendrimer molecule in order to slow down its diffusion *in vivo* (Fig. 1). The necessary synthetic transformations should yield a molecule bigger in size (*e.g.* an increase in the molecular weight), although the responsive part of the SCA must be retained, as well as its Ca-sensitivity and MRI activity. Furthermore, such a molecule would enable the delivery of a high local concentration of active species (SCA monomeric units), which is crucial for observing maximal MRI signal changes.[16]

For this purpose, we have prepared a reactive monomacrocyclic molecule that bears an ethylene glycol tetraacetic acid (EGTA)-derived Ca-chelator coupled to a 1,4,7,10-tetraazacyclododecane-1,4,7-tricarboxylic acid (DO3A) unit for Ca-sensing

[a] *MR Neuroimaging Agents Group, Max Planck Institute for Biological Cybernetics, 72076 Tübingen, Germany. E-mail: goran.angelovski@tuebingen.mpg.de*
[b] *Department for Physiology of Cognitive Processes, Max Planck Institute for Biological Cybernetics, 72076 Tübingen, Germany*
[c] *Molecular Imaging Center, National Institute of Radiological Sciences (NIRS), 4-9-1 Anagawa, Inage-ku, Chiba 263-8555, Japan*
[d] *Institute for Organic Chemistry, Faculty of Science, University of Tübingen, 72076 Tübingen, Germany*
[e] *Department of Imaging Science and Biomedical Engineering, University of Manchester, Manchester M13 9PT, UK*

† Electronic supplementary information (ESI) available: Methods, synthetic procedures, selected spectroscopic and MRI data. See DOI: 10.1039/c4cc07540d

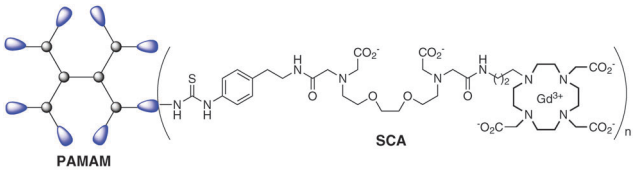

Fig. 1 Dendrimeric smart contrast agent **DSCA** consisting of a PAMAM G1 dendrimer coupled to Gd-complexes of a DO3A-unit bearing an EGTA-derived Ca-chelator.

and reporting purposes, respectively. This class of SCAs recently showed extremely advantageous properties, with both the mono- and bismacrocyclic SCA analogues exhibiting high r_1 changes in the presence of Ca^{2+}.[16,17] Moreover, studies in a complex cell culture model suggest that the T_1 change *in vivo* may exceed several percent, more than the current fMRI methodology allows. Furthermore, the SCA does not affect the normal cellular signaling, and Ca^{2+} transients persist even in its presence.

To allow the SCA coupling to the poly(amidoamine) (PAMAM) dendrimer, we have synthetically modified the EGTA-derived core and coupled an aryl-isothiocyanate (NCS) group to the terminus. The NCS group selectively reacts with the amine surface of the PAMAM dendrimer building a stable thiourea group, and this coupling reaction is a common choice for the preparation of dendrimeric MRI agents.[18,19] The synthetic route for the preparation of the desired dendrimer is shown in Scheme 1. The preparation commenced from amine **1** which was monoalkylated with benzyl chloride in the presence of cesium carbonate in dimethylformamide to obtain amine **2**. The macrocyclic bromide **3** that bears a DO3A chelator and the (propyl)acetamide linker was attached to amine **2** in the presence of potassium carbonate in acetonitrile to provide benzyl-protected amine **4**. The reductive removal of the benzyl group was achieved by $Pd(OH)_2$-catalyzed hydrogenation to yield amine **5**. The precursor **6** for the introduction of the NCS group was prepared by alkylation of 4-nitrophenylethylamine with bromoacetyl bromide. Amine **5** was subsequently alkylated with bromide **6** to obtain macrocycle **7**, which was used in two different reactions. The *tert*-butyl esters in the first portion of **7** were hydrolyzed with formic acid to give **8**, a chelator for Gd^{3+}. Upon preparation of **Gd8**, this complex was used to compare its r_1 response with the r_1 response of the desired dendrimeric SCA. Namely, **Gd8** already contains a Ca-chelator and can alone act as an SCA.

The nitro group in the second portion of **7** was reduced to the amine by Pd/C-catalyzed hydrogenation in ethanol to give aniline **9**. This was finally converted into isothiocyanate **10** using thiophosgene to obtain an amine-reactive SCA precursor that can be coupled to the PAMAM generation 1 (G1) dendrimer. The coupling of **10** to the dendrimer surface was achieved with triethylamine in dimethylformamide to obtain **11**. The product was purified by removing excess of unreacted **10** using a lipophilic Sephadex column with methanol as the eluent. The final dendrimeric ligand **12** was prepared by hydrolyzing *tert*-butyl esters with formic acid. The purification of **12** was performed by size-exclusion chromatography using a hydrophilic Sephadex column with water as the eluent. Dendrimer **12** was analyzed by ^{1}H NMR spectroscopy and MALDI-TOF/MS. The appearance of aromatic protons in the ^{1}H NMR spectrum is the evidence for NCS ligand-dendrimer conjugate formation (these peaks do not exist in the ^{1}H NMR spectra of the commercial PAMAM dendrimers). Gd^{3+} was introduced into DO3A chelators of the dendrimeric ligands using $GdCl_3 \cdot 6H_2O$ to obtain **DSCA**. Excess of Gd^{3+} from undesired complexation with the Ca-chelating part or the dendrimer core was removed using ethylenediaminetetraacetic acid (EDTA). The final product **DSCA** was purified by centrifugation

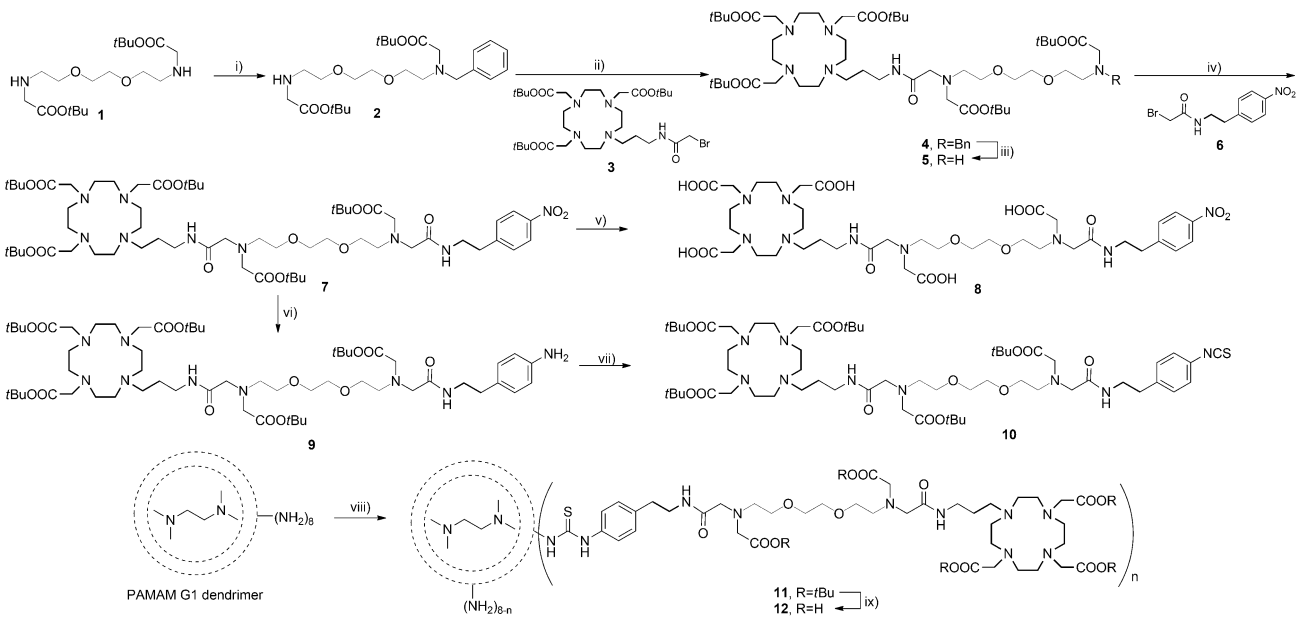

Scheme 1 Synthesis of dendrimeric SCAs. *Reagents and conditions*: (i) BnCl, Cs_2CO_3, CH_3CN, RT, 42%. (ii) **3**, K_2CO_3, CH_3CN, 70 °C, 71%. (iii) H_2, Pd/C, EtOH, RT, 95%. (iv) **6**, K_2CO_3, CH_3CN, 70 °C, 81%. (v) HCOOH, 60 °C, 81%. (vi) H_2, Pd/C, EtOH, RT, 97%. (vii) $CSCl_2$, Et_3N, RT, 58%. (viii) **10**, Et_3N, DMF, 45 °C, 77%. (ix) Formic acid, 60 °C, 97%.

using 3 KDa molecular weight cut-off filters to remove GdEDTA and excess of free EDTA, and was confirmed by MALDI-TOF/MS.

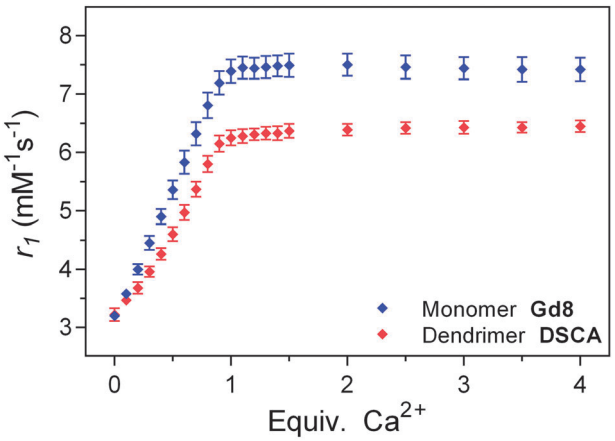

Fig. 2 Relaxometric titrations of **Gd8** and **DSCA** with Ca^{2+} at 7 T, 25 °C, pH 7.4 (HEPES). The r_1 values are represented as mean ± SD of three independent experiments, and are normalized to [Gd^{3+}] = 1.0 mM for both SCAs.

The activity of prepared monomeric **Gd8** and dendrimeric **DSCA** was investigated by relaxometric titrations at 7 T (300 MHz) and 25 °C in a buffered medium. Solutions of **Gd8** and **DSCA** with a known starting concentration of Gd^{3+} were prepared and the longitudinal T_1 relaxation times were determined upon addition of defined amounts of Ca^{2+}. The initial r_1 relaxivities of **Gd8** and **DSCA** were similar, showing that no gain in r_1 at high magnetic field (7 T) can be achieved for a Gd^{3+} complex with a large molecular weight.[20] Nevertheless, differences in the maximal r_1 enhancement were obtained upon saturation of the SCA solutions with Ca^{2+} (Fig. 2). **Gd8** and **DSCA** exhibited around 130% and 100% increase in r_1, respectively. These results are in line with our previous observations reported on SCAs with the same EGTA-derived Ca-chelator, but with different sizes and flexibilities.[17,21] The r_1 response in the flexible monomacrocyclic SCA is higher than in the sterically hindered bismacrocyclic SCA, which could be explained by reduced flexibility for intramolecular conformational changes in **DSCA**. However, it is very important to note that the high activity of monomeric SCAs incorporated in the dendrimeric system is retained. This opens a new realm of possibilities for attachment of NCS-containing monomeric SCAs to various nano-size carriers (*e.g.* functionalized

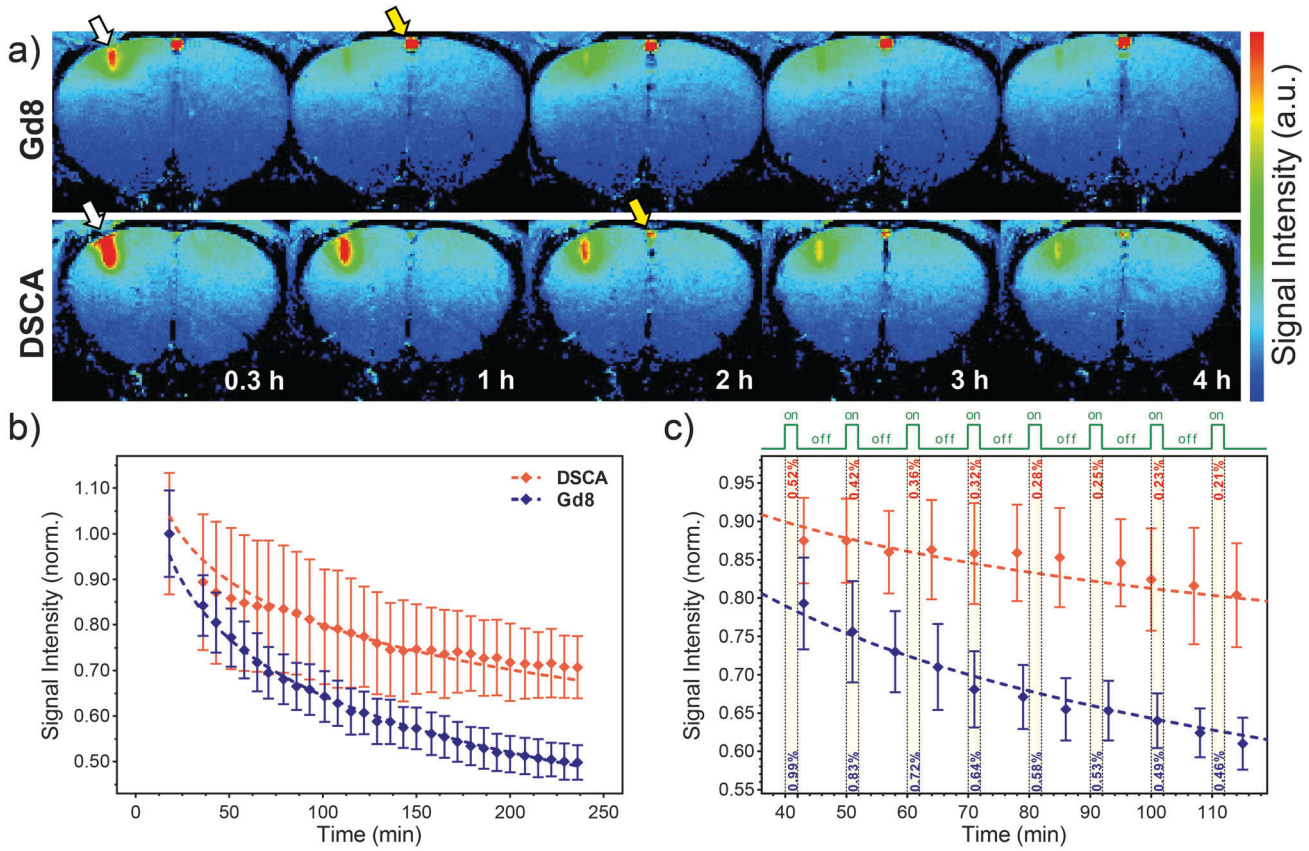

Fig. 3 *In vivo* MRI after **Gd8** or **DSCA** intracerebral administration. (a) Color-scaled typical T_1-weighted MR images 0.3, 1, 2, 3, and 4 h after SCA injection (upper: **Gd8**, lower: **DSCA**). White arrows indicate the injection site in the cortex. Yellow arrows show vessels on the surface of the brain. (b) Typical longitudinal signal alteration at the injection site after administration of **Gd8** (blue diamonds) and **DSCA** (red diamonds); dashed lines show logarithmic fits explained in the text and ESI.† ROIs (30 voxels) were defined around the injection site in the cortex (0.375 × 1.25 mm^2). (c) Selected regions from single experiments for small ROIs (9 voxels, 0.1–0.2 mm from the injection site), showing a decrease in the SI only due to diffusion of **Gd8** or **DSCA** during the hypothesized 2 min stimulation of the cortex (green line and yellow bars on the graph). Dashed lines show logarithmic fits performed for shown experimental points. Values for estimated SI changes were calculated from fits and shown within yellow bars.

dendrimers and nanoparticles), which should allow broader utilization of such responsive MRI probes.

The diffusion properties of **Gd8** and **DSCA** in the central nervous system (CNS) were investigated using MRI *in vivo*. **Gd8** or **DSCA** was administered into the rat cerebral cortex (the primary somatosensory forelimb region, S1FL). Twenty minutes after administration, thirty T_1-weighted MR images were acquired over a period of 4 hours (see ESI†). Although the **Gd8** injection site showed a robust signal increase in the cortex in 0.3 h, the signal enhancement rapidly attenuated after 1 h. In contrast, a larger signal increase was observed in the **DSCA**-injected region in 0.3 h, as compared to **Gd8**, and the signal enhancement was maintained over 3 h (Fig. 3a). The longitudinal changes in the SI for **Gd8** ($n = 3$) and **DSCA** ($n = 3$) were compared as a function of time. The SI in selected regions of interest (ROIs) from the SCA-injected sites in the cortex was normalized showing desired diffusion trends for **Gd8** and **DSCA** (Fig. 3b and ESI†). The SI of **DSCA** was significantly higher than that of **Gd8** at all time-points after injection. The slope of fitted logarithmic curves of **Gd8** (-0.18) was steeper than that of **DSCA** (-0.14). These results clearly indicate that the dendrimeric **DSCA** has a longer retention time in the CNS than the monomer **Gd8**.

The usefulness of this property was further estimated by a more specific analysis of MRI experiments. The maximal SI changes in dynamic, T_1-weighted fMRI experiments based on this concept are expected in regions with higher or similar SCA concentration relative to the local extracellular Ca-concentration ($[\mathrm{SCA}] \geq [\mathrm{Ca}^{2+}]_e$).[16] We therefore selected smaller ROIs closer to the injection site where higher SCA concentrations would be expected shortly after the intracerebral injection (40–90 min). The SI changes caused only by SCA diffusion were estimated every 10 min for a 2 min duration of a hypothesized 'stimulus-on' period (*e.g.* by performing trains of periodic electrical stimuli[5]). The results show an almost halved SI change of **DSCA** *vs.* **Gd8** due to diffusion, with the SI change always $<0.5\%$ for **DSCA** (Fig. 3c and ESI†). This is very encouraging because the loss of signal is still below the detection threshold valid for this type of experiment.[5] We note that at later time points the SI changes indeed become smaller, although the local SCA concentration also decreases below the level that may report the Ca^{2+} fluctuation changes.

In conclusion, we have developed a very useful technique to slow down the diffusion rate of SCAs and stabilize the measured SI during *in vivo* MRI in the CNS. The strategy we established allows synthetic modifications of the existing SCAs and their covalent attachment to functional nano-size carriers, while retaining their activity and bioresponsiveness. The resulting molecular probes allow more convenient functional imaging studies. The dynamic MRI with the use of responsive, slowly diffusing contrast agents holds great promise to visualize Ca-signaling during neuronal activity and may lead to valuable insights for understanding brain function.

The financial support from the Max-Planck Society, the Turkish Ministry of National Education (PhD fellowship to S.G.) and European COST CM1006 and TD1004 Actions is gratefully acknowledged. This research was partly supported by Kakenhi and Center of Innovation (COI) Program, Japan Science and Technology Agency (JST), Japan.

All animal experiments were approved by the Animal Welfare Committee of NIRS (07-1067-9) and were in full compliance with the Law for the Humane Treatment and Management of Animals (Law No. 105, Japan).

Notes and references

1 E. L. Que and C. J. Chang, *Chem. Soc. Rev.*, 2010, **39**, 51–60.
2 C. Q. Tu, E. A. Osborne and A. Y. Louie, *Ann. Biomed. Eng.*, 2011, **39**, 1335–1348.
3 M. C. Heffern, L. M. Matosziuk and T. J. Meade, *Chem. Rev.*, 2014, **114**, 4496–4539.
4 A. Y. Louie, M. M. Huber, E. T. Ahrens, U. Rothbacher, R. Moats, R. E. Jacobs, S. E. Fraser and T. J. Meade, *Nat. Biotechnol.*, 2000, **18**, 321–325.
5 T. Lee, L. X. Cai, V. S. Lelyveld, A. Hai and A. Jasanoff, *Science*, 2014, **344**, 533–535.
6 M. G. Shapiro, G. G. Westmeyer, P. A. Romero, J. O. Szablowski, B. Kuster, A. Shah, C. R. Otey, R. Langer, F. H. Arnold and A. Jasanoff, *Nat. Biotechnol.*, 2010, **28**, 264–270.
7 A. P. Koretsky, *NeuroImage*, 2012, **62**, 1208–1215.
8 A. Jasanoff, *Trends Neurosci.*, 2007, **30**, 603–610.
9 A. Jasanoff, *Curr. Opin. Neurobiol.*, 2007, **17**, 593–600.
10 E. Gianolio, R. Napolitano, F. Fedeli, F. Arena and S. Aime, *Chem. Commun.*, 2009, 6044–6046.
11 L. Frullano, C. Catana, T. Benner, A. D. Sherry and P. Caravan, *Angew. Chem., Int. Ed.*, 2010, **49**, 2382–2384.
12 E. Gianolio, L. Maciocco, D. Imperio, G. B. Giovenzana, F. Simonelli, K. Abbas, G. Bisi and S. Aime, *Chem. Commun.*, 2011, **47**, 1539–1541.
13 G. E. Hagberg, I. Mamedov, A. Power, M. Beyerlein, H. Merkle, V. G. Kiselev, K. Dhingra, V. Kubiček, G. Angelovski and N. K. Logothetis, *Contrast Media Mol. Imaging*, 2014, **9**, 71–82.
14 I. Mamedov, S. Canals, J. Henig, M. Beyerlein, Y. Murayama, H. A. Mayer, N. K. Logothetis and G. Angelovski, *ACS Chem. Neurosci.*, 2010, **1**, 819–828.
15 J. Henig, I. Mamedov, P. Fouskova, E. Tóth, N. K. Logothetis, G. Angelovski and H. A. Mayer, *Inorg. Chem.*, 2011, **50**, 6472–6481.
16 G. Angelovski, S. Gottschalk, M. Milošević, J. Engelmann, G. E. Hagberg, P. Kadjane, P. Andjus and N. K. Logothetis, *ACS Chem. Neurosci.*, 2014, **5**, 360–369.
17 P. Kadjane, C. Platas-Iglesias, P. Boehm-Sturm, V. Truffault, G. E. Hagberg, M. Hoehn, N. K. Logothetis and G. Angelovski, *Chem. – Eur. J.*, 2014, **20**, 7351–7362.
18 C. A. Boswell, P. K. Eck, C. A. S. Regino, M. Bernardo, K. J. Wong, D. E. Milenic, P. L. Choyke and M. W. Brechbiel, *Mol. Pharmaceutics*, 2008, **5**, 527–539.
19 M. M. Ali, M. Woods, P. Caravan, A. C. L. Opina, M. Spiller, J. C. Fettinger and A. D. Sherry, *Chem. – Eur. J.*, 2008, **14**, 7250–7258.
20 J. B. Livramento, C. Weidensteiner, M. I. M. Prata, P. R. Allegrini, C. Geraldes, L. Helm, R. Kneuer, A. E. Merbach, A. C. Santos, P. Schmidt and E. Toth, *Contrast Media Mol. Imaging*, 2006, **1**, 30–39.
21 G. Angelovski, P. Fouskova, I. Mamedov, S. Canals, E. Toth and N. K. Logothetis, *ChemBioChem*, 2008, **9**, 1729–1734.